

## Article

# Some Unmodified Household Adsorbents for the Adsorption of Benzalkonium Chloride—A Kinetic and Thermodynamic Case Study for Commercially Available Paper

Enikő Bitay<sup>1,2,3</sup>  and Alexandra Csavdari<sup>4,5,\*</sup>

- <sup>1</sup> Department of Mechanical Engineering, Faculty of Technical and Human Sciences, Sapientia Hungarian University of Transylvania, Calea Sighișoarei 2, 540485 Târgu-Mureș, Romania
- <sup>2</sup> Bánki Donát Faculty of Mechanical and Safety Engineering, Óbuda University, Népszínház Street 8, 1081 Budapest, Hungary
- <sup>3</sup> Research Institute of the Transylvanian Museum Society, Napoca Street 2-4, 400009 Cluj-Napoca, Romania
- <sup>4</sup> Department of Chemical Engineering, Babeș-Bolyai University of Cluj-Napoca, Arany Janos Street 11, 400028 Cluj-Napoca, Romania
- <sup>5</sup> Department of Analytical, Colloidal Chemistry and Technology of Rare Elements, Al-Farabi Kazakh National University, 71 Al-Farabi Avenue, Almaty 050040, Republic of Kazakhstan
- \* Correspondence: alexandra.csavdari@ubbcluj.ro

**Abstract:** The extensive use of biocide surfactant benzalkonium chloride (BAC) during the SARS-CoV-2 pandemic has led to the buildup of this hazardous chemical in waste, surface and groundwater. The study aims to elucidate whether various low-cost household materials are suitable, in their unmodified and untreated form, to effectively adsorb BAC from its aqueous solutions. Additionally, if a proper adsorbent is identified, a description of the kinetics and thermodynamics of the process is also targeted. From among the five tested materials, a commercially available white household paper towel was chosen to best satisfy the criteria of low price, large availability, and standardization degree, as well as high adsorption capacity within a fairly short time window needed until equilibrium. Batch experiments were carried out with a commercial mixture of BAC-12 and BAC-14 within a temperature range of 18–45 degrees Celsius, and a 25–100 mg/g BAC/adsorbent initial mass ratio range, respectively. The overall process follows a pseudo-second-order kinetic law, with an apparent activation energy of 73.35 KJ/mole. Both the Langmuir and the Redlich–Peterson isotherms describe the equilibrium data at 298 K well, with a Gibbs free energy of  $-20.64$  KJ/mole. These findings are in agreement with previous reports and suggest a hybrid but chemisorption-dominated process.

**Keywords:** benzalkonium chloride; adsorption; unmodified adsorbents; household paper; pseudo-second-order kinetic law; chemisorption-dominated process



**Citation:** Bitay, E.; Csavdari, A. Some Unmodified Household Adsorbents for the Adsorption of Benzalkonium Chloride—A Kinetic and Thermodynamic Case Study for Commercially Available Paper. *Toxics* **2023**, *11*, 950. <https://doi.org/10.3390/toxics11120950>

Academic Editors: Yuezhou Wei, Yan Wu and Xinpeng Wang

Received: 1 November 2023

Revised: 12 November 2023

Accepted: 15 November 2023

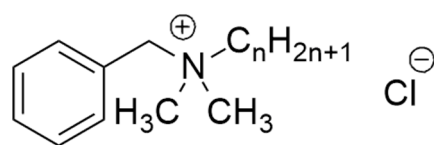
Published: 21 November 2023



**Copyright:** © 2023 by the authors. Licensee MDPI, Basel, Switzerland. This article is an open access article distributed under the terms and conditions of the Creative Commons Attribution (CC BY) license (<https://creativecommons.org/licenses/by/4.0/>).

## 1. Introduction

Benzalkonium chloride (BAC) is a quaternary ammonium salt used mainly as a cationic surfactant with a broad anti-microbial spectrum. It may be observed from the structural formula illustrated in Scheme 1 that it contains a benzyl group, two methyl groups, and an alkyl group. The latter has a varying from 8 to 18, even-numbered carbon atom chain length. The commercially available formulation is usually a 50%wt aqueous BAC solution, containing a mixture of 12 and 14 carbon atom chains in different but usually equal ratios.



**Scheme 1.** The structural formula of benzalkonium chloride (BAC), where  $n = 8 \div 18$  stands for the even number of carbon atoms in the chain of the alkyl group.

One of the drivers of its increasing market importance since the recent SARS-CoV-2-caused pandemic is the widespread use of BAC-containing hand sanitizers and surface disinfectants as alternatives to alcohol-based products. As a result, its market value reached USD 715.064 million in 2020 and is expected to grow by 8.7% by 2027 [1]. Although very effective for the purpose it has been designed for, BAC might accumulate in municipal or other wastewaters. Despite some efforts to inhibit its action or to biodegrade it [2,3], the usual corresponding wastewater treatment plants are not fully designed to deal with this species [4–6]. Hence, it may reach various natural environments and build up in wastewater influents and/or effluents, surface and groundwater, respectively [6], and as such, raise ecological concerns [7–12].

Although there is no official threshold limit for the legally allowed benzalkonium chloride content of surface, waste, and/or groundwater, chemical companies mention 96 h LC50 values for various fish in the range of ppm concentrations in the aquatic media [13,14]:  $0.223 \div 0.46$  mg/L for *Lepomis macrochirus*;  $0.823 \div 1.61$  mg/L for *Oncorhynchus mykiss*; 1.3 mg/L for *Poecilia reticulata*; and 2.4 mg/L for *Oryzias latipes*. Material safety sheets state that it is “very toxic to aquatic life” [14,15] and recommend that users avoid BAC discharge in lakes, streams, and sewers [15] and contact the environmental authorities in case of accidental leakages [15]. Fuchsman *et al.* [7] express the opinion that even though BAC-12 and BAC-14 (BAC species in Scheme 1, with  $n = 12$  and 14) are the most prevalent BAC compounds in wastewater influents, they generally “exhibit low bioaccumulation potential, tending to be retained on epithelial surfaces rather than crossing cell membranes”. Hence, it is more likely for BAC-16 and BAC-18 (BAC species in Scheme 1, with  $n = 14$  and 16) to be found in fish tissue [7].

It has been reported that BAC has a neurotoxic effect on zebrafish (*Danio rerio*). Sousa *et al.* [12] reported increasing overall swimming activity, thigmotaxis behavior, and erratic movements, whereas Sreevidya *et al.* [8] observed hatching delay or the inhibition of embryos, embryo enhanced mortality, and the prevalence of morphological malformations, with acute toxicity occurring at concentrations of hundreds of  $\mu\text{g/L}$ . Ikisa *et al.* [9] observed a direct positive relationship between *O. niloticus* juvenile mortality and BAC concentration in freshwater. BAC also induced relevant DNA damage, thus proving its genotoxicity, in both *Daphnia magna* and *Ceriodaphnia dubia* [10], with acute effects occurring at tens of  $\mu\text{g/L}$  in *D. magna* and hundreds of  $\mu\text{g/L}$  in *C. dubia*, respectively. On the other hand, comparable ranges of BAC concentrations of 15 to 200  $\mu\text{g/L}$  did not significantly affect the physiological variables of *Isochrysis galbana* and *Chaetoceros gracilis* microalgae batch cultures, nor those of a coastal phytoplankton assemblage [11].

Tezel *et al.* [16] proved that at these low concentrations, counter-ions such as bromide, nitrate, and acetate did not affect the bioavailability, hence the toxicity of BAC, even if present in three-fold higher-order-of-magnitude concentrations. Yet, similar quantities of natural organic matter somewhat reduced the biocide’s toxicity. Reported environmentally relevant surface and freshwater BAC concentrations may vary from units of  $\mu\text{g/L}$  [10] to hundreds of  $\mu\text{g/L}$  [11,12], with levels inducing adverse effects or acute toxicity, depending on the examined species, anywhere within this range. Therefore, environmental risk issues created by the wide and intensive use of benzalkonium chloride may not be ignored when striving for the preservation of a safe and healthy environment [6].

Adsorption is one of the most versatile, efficient, and fairly low-cost methods to mitigate polluted waters from a wide variety of species [17,18], ranging from heavy metals [19] to cationic and/or anionic dyes [20,21]. Some studies have endeavored to use readily available low-cost adsorbents, such as sawdust [22–24], cardboard [24], or paper [25,26], whereas others have reported specifically designed ones in order to target certain adsorbates [27–29].

The removal of benzalkonium chloride from aqueous solutions by means of adsorption is also mentioned in the literature. One of the earliest studies reported that its adsorption on activated granular carbon [30] is controlled by intraparticle diffusion and characterized at equilibrium by a Freundlich isotherm. A decade ago, Zanini *et al.* [31] proposed the use of montmorillonite as an adsorbent and compared the adsorptions of BAC-12 and BAC-14,

respectively. Both BAC variants exhibited two distinct stages in the isotherm, the one at lower pollutant concentrations corresponding almost exclusively to a cation exchange process, whereas the one at higher concentrations was considered to be mainly driven by lateral interactions between the surfactant BAC molecules. These studies were continued by adding triclosan, another biocide, to the pollutant's mixture, as well as by putting forward a Langmuir isotherm for the binary adsorption model [32]. BAC's competitive adsorption with a herbicide on the same adsorbent was assessed by means of a theoretical cation exchange model [33]. A laboratory-synthesized magnetite nanomaterial was also tried recently [34]. Again, a Langmuir isotherm described very well the experimental data.

Other types of BAC adsorbents include polymers. Both an acrylic ester, and a styrenic polymer were used to remove it from aqueous streams in a single adsorbent column [35]. Similar to previous findings [30], intraparticle mass transfer was considered to significantly affect the process rate. However, concerning the mechanism, the interaction between the adsorbent and adsorbate indicated slightly exothermic physical sorption [35]. The adsorption of three BAC variants (BAC-12, BAC-14, and BAC-16) on polyethylene microplastics, as well as their combined toxic effects on *Daphnia magna*, were assessed by using batch experiments [36]. Overall, pseudo-second-order kinetic laws were further proposed.

More detailed adsorption mechanisms involving various alkyl group chain length BACs were carried out just recently [37]. The adsorption of BAC-12, BAC-14 and BAC-16, respectively, from aqueous media on powdered activated carbon showed that species with longer alkyl chains were adsorbed more effectively. Therefore, electrostatic interaction is more significant in BAC-12 adsorption, whereas for the other two species, van der Waals interaction plays a more important role. In all cases, pseudo-second-order kinetics and Langmuir isotherms proved to best fit the experimental data.

BAC adsorption was employed for other purposes: to probe the montmorillonite surface reactivity when encapsulated in a composite of alginate hydrogels [38], to decide whether zeolite–surfactant–drug composites are suitable drug deliverers when BAC is co-adsorbed with sulfamethoxazole on purified natural clinoptilolite [39], or to choose the best sterilizing grade filter membranes in the pharmaceutical industry, so that they retain the least BAC possible, and its concentration in the filtrate does not drop below its predetermined specification sterile limit [40,41].

It may be concluded that although there was some preoccupation for benzalkonium chloride removal from various water samples by means of adsorption, research efforts have mostly concentrated on finding the process conditions (temperature, pH, mixing rate, adsorbate/adsorbent mass ratio, ionic strength, process time, etc.) that ensure the most effective BAC elimination. Furthermore, various process mechanisms and isotherm models have been proposed, whereas detailed kinetic aspects have rarely been addressed, almost entirely since the SARS-CoV-2 pandemic. Except for the filtering membranes, which were acquired from commercial sources, all other adsorbents mentioned in the literature were subjected to some physical or chemical treatment prior to the adsorption experiments.

Therefore, this work aims to test the suitability of low-cost, unmodified adsorbents for BAC among various household items. The proposed material ought to be employed effectively in its available form, either from commercial sources or waste. Additionally, supplementary experiments are planned concerning the suitable candidate in order to conclude upon a more detailed kinetic model of the overall process, as well as to put forward an isotherm equation that best explains the adsorption mechanism under the employed conditions.

## 2. Materials and Methods

A commercially available 50 wt% aqueous solution of benzalkonium chloride, containing a mixture of BAC-12 and BAC-14 in an unspecified ratio, was provided by *SC Grande Gloria SRL*, Galați, Romania and used as the source of a 5 g/L BAC stock solution. This was employed both in calibration (absorbance *vs.* BAC concentration) as well as in the adsorption experiments. All were carried out with deionized and double distilled water.

The following adsorbents were chosen from easily accessible sources: *Expertto* white household paper towel (*SC Grande Gloria SRL*, Galați, Romania), *“Anna” Soft and Delicate* light blue viscose household cloth (*Stella Pack S.A.*, Lubartów, Poland), white tea filter paper (*Demmer GmbH*, Wien, Austria), white cotton string (*Românofir S.A.*, Tâlmăciu, Romania), and a mixture of oak and beech sawdust from a private mountain farm in Brașov County, Romania, respectively.

The adsorbent's relative humidity was determined *via* gravimetric measurements (*Kern ABT220-5DNM* analytical scale) by drying samples of 20 g (*Memmert UN30* drying chamber) at 105 °C for 24 h and was assessed as a percentage of the mass before drying. The bulk density of dry sawdust was determined *via* the triplicate weighting of 200 mL solid. All adsorbents were employed in experiments in the form provided by their respective commercial sources, except the sawdust, which was dried first. No other physical or chemical treatment prior to the BAC adsorption experiments was employed.

Benzalkonium chloride adsorption experiments were carried out in batch arrangements by using 150 mL covered glass recipients in order to limit water evaporation during the course of the experiments. Each water–BAC–adsorbent mixture was prepared in triplicate in a 50 mL aqueous solution of 500 mg/L BAC. The start of the process was operationally defined by the moment at which a weighted amount of solid adsorbent was placed into the BAC solution. The variation of the initial adsorbate/adsorbent mass ratio in five steps, from 25 to 100 mg/g, was achieved by varying the mass of adsorbent placed into the recipients. The temperature was kept constant by pre-warming all of the employed materials and keeping the glasses in a thermostated drying chamber.

No stirring was employed during the experiments other than the rapid mixing of the sample when placing the adsorbent into it. The authors considered that such an approach might resemble the slow passing of wastewater through a filter.

At predetermined time intervals, varying from 30 min to 1–2 days, 3 mL aliquots of the liquid bulk solution were extracted in order to record their absorbance at 262 nm (*Jasco V-650 UV-VIS* spectrophotometer) by using quartz cuvettes of 1 cm optical path length. When 3 consecutive values did not vary for more than 2%, adsorption equilibrium was considered to be achieved. These aliquots were re-added to their corresponding mixtures in order to keep the liquid bulk's volume constant during the experiment.

The remnant BAC concentration was calculated from the absorbance *vs.* BAC concentration Lambert-Beer calibration line. This was obtained by using 10 triplicate aqueous biocide solutions in the concentration range of 100 to 2500 mg/L BAC.

Necessary calculus has been carried out by using Microsoft Office Excel and its Data Analysis toolpak, as well as the MatLab Software (Version 2021 A).

### 3. Results and Discussion

#### 3.1. Choice of Adsorbent

The five different adsorbent candidates were compared by means of the following criteria in order to choose the most suitable one for further studies:

1. Low price and easy availability (commercial sources);
2. Good standardization (already ensured by the producer);
3. An approximately zero value for the 262 nm absorbance of the adsorbent-water mixture, so that it does not interfere with the values provided by BAC;
4. A high equilibrium adsorption yield coupled with a low total S-L contact time required until equilibrium.

The first three criteria are summarized in Table 1. Prices were estimated by using the Romanian local currency conversion rate into EUR as of 30 October 2023. For the outer surface, only the apparent surface of both sides of a cloth or a sheet of paper is taken into account. It is not to be mistaken for the total surface available for adsorption, which also includes the inner surface of the pores. As such, the values in Table 1 were assessed *via* calculation from the geometrical size and weight measurements of one cloth, one sheet of household paper, and one tea filter, respectively. The parameter has no practical

value except for being a helpful tool in assessing the standardization quality ensured by the producer. The same is true for the relative humidity. The listed absorbance at 262 nm represents the average value registered for five distinct mixtures within the range of 2.5–25 g/L solid adsorbent in water.

**Table 1.** Comparison among solid BAC adsorbent candidates in terms of price, availability, standardization degree and 262 nm absorbance value in water.

Adsorbent	Price (EUR/kg)	Availability	Standardization Degree <sup>1</sup>	Absorbance at 262 nm
White household paper towel	7.5	Easy (retail)	<ul style="list-style-type: none"> <li>– Controlled and constant quality ensured by the producer;</li> <li>– <math>(42.68 \pm 0.18)</math> g/m<sup>2</sup> outer surface;</li> <li>– <math>(6.42 \pm 0.24)</math>% relative humidity.</li> </ul>	$0.015 \pm 0.012$
Light blue viscose household cloth	30.2	Easy (retail)	<ul style="list-style-type: none"> <li>– 70% viscose, 30% polyester <sup>2</sup>;</li> <li>– Controlled and constant quality ensured by the producer;</li> <li>– Approximately 18.9 g/m<sup>2</sup> outer surface.</li> </ul>	$0.018 \pm 0.009$
White tea filter paper	82.2	Easy (retail)	<ul style="list-style-type: none"> <li>– Controlled and constant quality ensured by the producer;</li> <li>– <math>(16.99 \pm 0.05)</math> g/m<sup>2</sup> outer surface;</li> <li>– <math>(4.31 \pm 0.17)</math>% relative humidity.</li> </ul>	$0.018 \pm 0.008$
White cotton string	16.7	Easy (retail)	<ul style="list-style-type: none"> <li>– Controlled and constant quality ensured by the producer;</li> <li>– Thickness<sup>2</sup> of 1 mm;</li> <li>– Approximately<sup>2</sup> 250 g/100 m.</li> </ul>	$0.003 \pm 0.003$
Sawdust	0.16	Easy (household)	<ul style="list-style-type: none"> <li>– Quality and composition dependent on source;</li> <li>– Approximately 24% relative humidity;</li> <li>– <math>(254.5 \pm 3.8)</math> g/L dry bulk density.</li> </ul>	From 0.38 to 3.60

<sup>1</sup> As ensured by the producer. <sup>2</sup> As indicated by the producer.

Figure 1 sheds light on the choice of the use of a 262 nm wavelength to monitor the absorbance of the liquid phase in order to assess its remaining BAC content. Curve (a) corresponds to the UV spectrum of a 500 mg/L aqueous BAC solution. It has three peaks, at 268, 262 and 257 nm, respectively, with the one at 262 nm being the highest. Therefore, it was chosen for the purpose of quantifying BAC concentrations from the absorbance measurements as long as the adsorbent does not add to the A value. This is exactly the case with the white household paper towel. Its UV spectrum is illustrated in curve (b), and shows the negligible value of  $A = 0.0136$  at 262 nm. Curve (c) illustrates the spectrum of the aqueous bulk phase of an initially 500 mg/L BAC solution containing 10 g/L paper at adsorption equilibrium (after 48 h of total S-L contact time). It may be observed that (i) the shape of the spectrum is similar to that of curve (a), demonstrating that the adsorbent does not affect A values, and (ii) the peak at 262 nm can be correlated with the remaining BAC content in the liquid phase. As a result, the difference of absorbance A at 262 nm between curves (a) and (c) is directly correlated with the adsorbed BAC. Methods relying on spectrophotometric determination of BAC use the same wavelength of 262 nm in UV [37] or a close one of 215 nm in the far-UV [41].

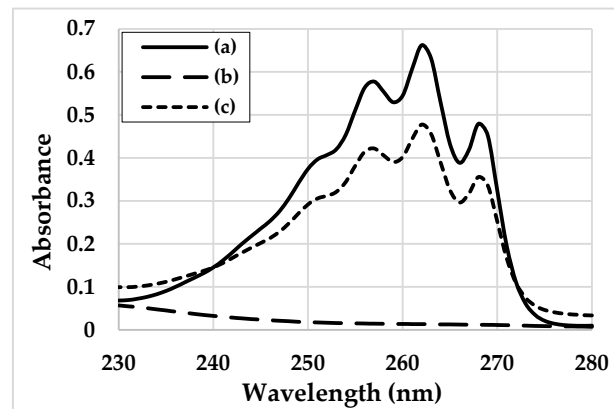


**Figure 1.** UV absorbance spectrum of the liquid phase for (a) a 500 mg/L aqueous BAC solution, (b) a water-paper mixture containing 10 g/L paper, and (c) a water-BAC-paper mixture containing initially 500 mg/L BAC and 10 g/L paper, at adsorption equilibrium and at  $18.0 \pm 0.1$  °C, respectively.

The data in Table 1 indicate sawdust as the first choice in terms of price. However, it presents the disadvantage of needing standardization as well as having a significant absorbance signal at 262 nm. This is due to some extraction–dissolution processes of organic species from sawdust [42,43]. Hence, it might interfere with the determination of BAC concentrations *via* spectrophotometric measurements and could potentially interfere with the BAC adsorption process. The next best option is the household paper towel. It has a reasonable price, the producer ensures a good standardization quality, and no other species interferes with BAC concentration determinations at 262 nm or with its adsorption.

Criterion 4 in the list above was assessed by using the equilibrium 262 nm absorbance values of the aqueous bulk solutions,  $A_{eq}$ , of the water–BAC–adsorbent mixtures, as well as the corresponding  $A_0$  values of BAC aqueous solutions of the same concentration as the tests' initial ones. In this study, 10 g/L of each adsorbent was employed for  $C_{BAC}^0 = 1000$  mg/L initial BAC concentrations at  $18.0 \pm 0.1$  °C. The adsorption equilibrium yield  $\eta_{eq}$  (%) was calculated by means of Equation (1). Equilibrium was considered to be achieved when three consecutive absorbance measurements (at different total S-L contact times) did not vary for more than 2%. Figure 2a,b illustrate the results registered during the assessment of criterion 4 for the choice of the most suitable BAC adsorbent.

$$\eta_{eq} = \frac{A_0 - A_{eq}}{A_0} \times 100 \quad (1)$$

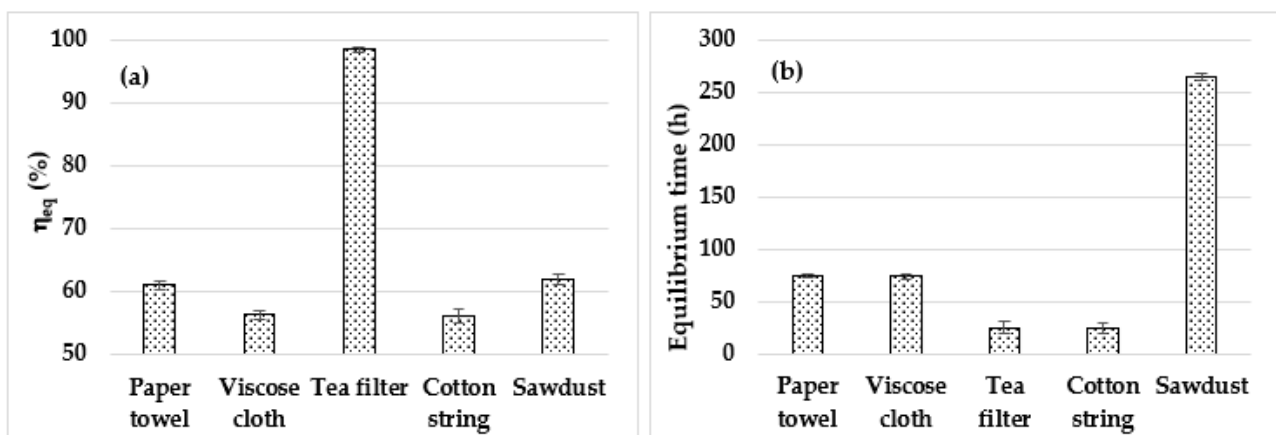


**Figure 2.** (a) Values of the equilibrium adsorption yield; (b) total S-L contact time until equilibrium. Data describe the 5 different employed adsorbents, with corresponding error bars for triplicate determinations, at 50 mg/g BAC/adsorbent initial mass ratio and  $18.0 \pm 0.1$  °C, respectively.

The calculus for  $\eta_{eq}$  was carried out with absorbance values instead of BAC concentrations because not all adsorbents have negligible  $A_{262}$  values in aqueous media, see sawdust, for example. The first four adsorbents in Table 1 do not add to the overall absorbance value at 262 nm, and the A values in Equation (1) are only due to the presence of BAC. Hence, the corresponding  $\eta_{eq}$  values of these adsorbents in Figure 2a are pertinent.

On the other hand, since the sawdust itself contributes to any  $A_{262}$  value registered for the bulk liquid phase, the  $A_{eq}$  value of the sawdust–BAC mixtures contains contributions from both species. As a result, the numerator ( $A_0 - A_{eq}$ ) in Equation (1) is not quantitatively linked with the remaining liquid phase BAC concentration at equilibrium. Hence, the value of  $\eta_{eq}$  for sawdust in Figure 2a ought to be regarded with reservations.

According to the data presented in Figure 2, the most suitable adsorbent that satisfies criterion 4 above is tea filter paper. In 4 h, it reaches an approximately 80% adsorption yield, and in 24, almost 100%. The next suitable choices would be cotton string, household paper towel and household viscose cloth, in this order. Yet, the cheapest among these is the towel. According to the data in Table 1, it also would be a good choice.

Hence, the white household paper towel provided by *Expertto (SC Grande Gloria SRL, Galați, Romania)* was chosen for further BAC batch adsorption experiments for the purpose of establishing the kinetic and thermodynamic aspects of this process.

### 3.2. Experimental Data and Their Processing Method

The BAC adsorption experiments from its synthetic aqueous solutions on solid household paper towels were carried out, as described in Section 2. The one variable at a time approach was used. Firstly, the temperature varied stepwise at constant initial BAC and adsorbent contents in the mixtures (constant adsorbate/adsorbent initial mass ratio). Then, the temperature was kept constant at  $25.0 \pm 0.1$  °C, and the adsorbate/adsorbent initial mass ratio varied stepwise. These data ought to elucidate the process thermodynamics and serve for the calculus of the equilibrium constant at 25 °C, the standard temperature.

Since, in all cases, the absorbance values were recorded at predetermined values of time, more often after the initiation of the process and less often towards the equilibrium, all data serve for the elucidation of process kinetics, as well as for the calculus of overall rate coefficients.

A calibration line absorbance *vs.*  $C_{BAC}$  was obtained at 262 nm in order to link the absorbance of the liquid phase bulk with the remaining, un-adsorbed BAC concentration. Its mathematical expression is provided in Equation (2), where  $C_{BAC}$  is expressed in mg/L.

$$A_{262} = (0.071 \pm 0.014) + (1.184 \pm 0.011) \times 10^{-3} C_{BAC} \quad (2)$$

The  $R^2_{adjusted} = 0.9974$  value demonstrates the good quality of the calibration. The slope permits the calculus of the molar absorption coefficient for known BAC variants. Because BAC solutions have been prepared from a commercial source with an unspecified BAC-12 and BAC-14 ratio, concentrations are expressed in “overall” mg/L BAC instead of mole/L. Therefore, the slope of Equation (2) is expressed in  $(\text{mg/L})^{-1} \cdot \text{cm}^{-1}$ .

For correct  $C_{BAC}$  calculus, the  $A_{262}$  values used in Equation (2) were corrected by subtracting the adsorbent’s own absorbance (of an average value of 0.015 as listed in Table 1) from the one of the test’s mixture.

Further,  $C_{BAC}$  values served to calculate the adsorption capacity  $q$  (mg/g), according to Equation (3).  $C^0_{BAC}$  (mg/L) stands for the initial concentration of BAC, whereas  $C_{BAC}$  (mg/L) stands for the one at a certain moment  $t$  after process initiation, respectively.  $C_{adsorbent}$  (g/L) is the adsorbent content of the aqueous BAC–solid adsorbent mixture. Hence,  $q$  stands for the mass (mg) of BAC adsorbed by 1 g of adsorbent after a certain S-L contact time  $t$ .

$$q = \frac{C^0_{BAC} - C_{BAC}}{C_{adsorbent}} \quad (3)$$

The equilibrium value of  $q$  is represented by  $q_{eq}$  and was determined experimentally in each case.

Figure 3a presents a set of typical results of calculus with Equation (3) in the form of the adsorption capacity  $q$  vs. total S-L contact time profile at  $25.0 \pm 0.1$  °C and 50 mg/g initial BAC/household paper towel mass ratio. The star symbols stand for all of the data derived from the triplicate experiments. Negligible differences among the triplicates may be observed ( $RSD < 5\%$ ). The data show that approximately 90% of the process occurs within the first 5 h, with dramatic  $q$  value increases. Yet, equilibrium is attained far more slowly, taking about three or more days. These findings are in agreement with the data reported in the literature [31,36,37].

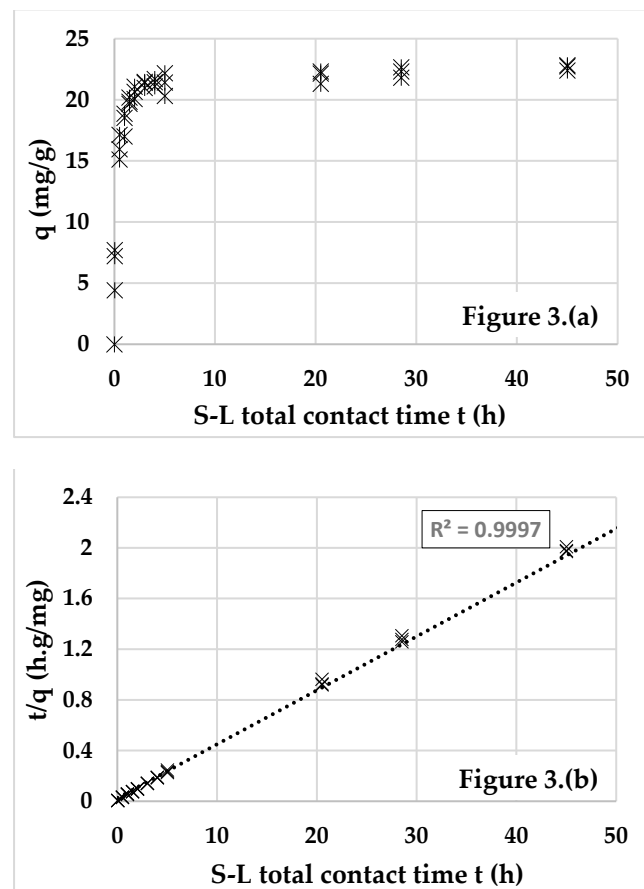


**Figure 3.** Example of adsorption capacity  $q$  vs. total S-L contact time plot (a), and the corresponding plot of the linearized pseudo-second-order kinetic law (b). Data for 50 mg/g initial BAC/paper mass ratio, at  $25.0 \pm 0.1$  °C.

The first line of experiments was carried out at 18, 25, 35 and 45 °C, respectively, by keeping the starting BAC/paper mass ratio at constant 50 mg/g. The second line of trials kept the temperature constant at 25 °C, and varied the initial adsorbate/adsorbent mass ratio by giving it values of 25, 37.5, 50, 75 and 100 mg/g, respectively. In all cases, similar curves to the one depicted in Figure 3a were obtained, with significantly shorter time frames necessary until equilibrium at higher temperatures.

Single-factor ANOVA statistical testing was employed in order to assess whether the  $q = f(\text{time})$  profiles like the one in Figure 3a were statistically significantly affected by the variation of either the temperature or the initial adsorbate/adsorbent mass ratio. Calculus was performed by using the Data Analysis toolpak of Microsoft Office Excel.

Statistical testing based on analysis of variance (ANOVA) is a technique that allows the isolation and estimation of variations between various data sets. It further classifies

the differences as statistically “significant” or “insignificant”, depending on the value of the Fisher criterion (the F value). If its value exceeds the  $F_{\text{significance}}$  threshold, then the differences are statistically significant [44] (pp. 59–65). Otherwise, they are statistically insignificant. The threshold value depends on the number of degrees of freedom, which, in turn, is related to the number of experimental data subjected to testing.

For the effect of temperature, the value of the Fisher criterion was found to be equal to 17.62, higher than the threshold  $F_{\text{significance}} = 2.68$ . Similar results were obtained for the effect of the initial BAC/paper mass ratio, with  $F = 1874.4$  being much higher than  $F_{\text{significance}} = 2.41$ . The results show that both parameters affect statistically significantly the course and outcome of the adsorption process, yet with a far more dramatic influence by initial conditions than the temperature (at least within the range of employed process conditions).

### 3.3. Process Kinetics

The  $q = f(\text{time})$  profiles obtained *via* the above-described means have been tested against the pseudo-first, pseudo-second, and intra-particle diffusion models described by Yagub *et al.* [21], as well as against a more detailed kinetic model consisting of two parallel competing first-order individual stages [45]. The only fit was the one describing a pseudo-second-order overall adsorption process. According to it, the value of  $q$  follows a hyperbolic profile until it reaches the equilibrium value  $q_{\text{eq}}$ , see Figure 3a, with a pseudo-second-order kinetic rate coefficient  $k$  expressed in (g/mg·h), see Equation (4).

$$\frac{dq}{dt} = k(q_{\text{eq}} - q)^2 \quad (4)$$

Its linear form (5) permits the calculus of both the rate coefficient  $k$  and the equilibrium adsorption capacity  $q_{\text{eq}}$ , from the intercept and slope of the linear plot of the  $(t/q)$  values against  $t$ . Figure 3b presents this for the data shown in Figure 3a. Good linearization is observed, proving the suitability of the chosen kinetic model.

$$\frac{t}{q} = \frac{1}{kq_{\text{eq}}^2} + \frac{1}{q_{\text{eq}}}t \quad (5)$$

The plot in Figure 3b enabled the calculation of  $q_{\text{eq}} = 23.53$  mg/g, which is practically equal to the experimental 23.56 mg/g value (see also Table 3). Similar matches were found for the other employed experimental conditions. This fact is a further argument in favor of the kinetic model described in Equation (4). Such findings are in agreement with previously reported ones [36,37].

Equation (5) was used to determine adsorption rate coefficients for three more adsorbents of Table 1: household viscose cloth, tea filter paper, and cotton string, respectively, at  $18.0 \pm 0.1$  °C and 50 mg/g adsorbate/adsorbent initial mass ratio. For these species, the calculus algorithm, described in Section 3.2, was also suitable because the adsorbent did not contribute to the overall absorbance value of the bulk liquid phase at 262 nm. The results are summarized in Figure 4 and are in good correlation with those presented in Figure 2b, supporting the decision favoring the use of this paper towel as a suitable BAC absorbent.

Table 2 contains the calculated pseudo-second-order rate coefficients  $k$  as a function of the employed temperature,  $T$ , as well as the statistical  $R^2_{\text{adjusted}}$  values of the linear regressions from which they were calculated, such as the one in Figure 3b. The last column proves the good quality of the (i) experimental data and (ii) linearizations, hence model fit.

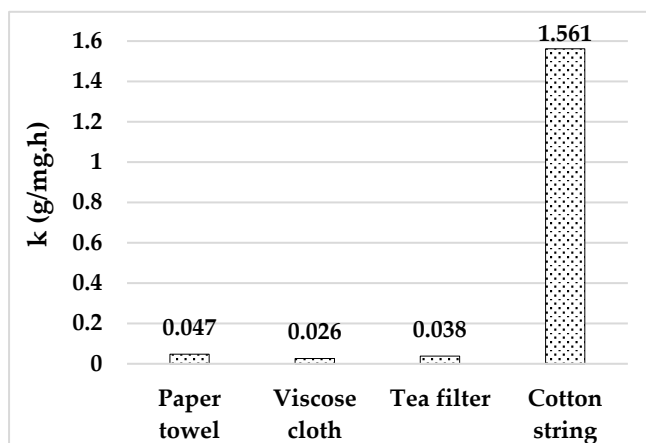


**Figure 4.** Pseudo-second-order rate coefficients *k* for various adsorbents at 18.0 ± 0.1 °C and 50 mg/g initial BAC/adsorbent mass ratio.

**Table 2.** Pseudo-second-order rate coefficients *k* as a function of temperature, at 50 mg/g initial BAC/household paper towel mass ratio.

T (K)	100 × <i>k</i> (g/mg·h)	R <sup>2</sup> <sub>adjusted</sub>
291 ± 0.1	4.74 ± 0.08	0.9932
298 ± 0.1	7.00 ± 0.23	0.9997
308 ± 0.1	10.44 ± 0.17	0.9971
318 ± 0.1	72.93 ± 1.68	0.9889

R<sup>2</sup><sub>adjusted</sub> is a strong statistical tool when comparing models with different numbers of independent variables *m* and data points *n*. Therefore, it is a better indicator of model quality than the simple R<sup>2</sup>, because it shows the variability in the target variable due only to independent variables that actually affect it [44] (pp. 92–108), [46,47]. The relationship between these two statistical parameters is described in Equation (6). It may be observed that, for the same *m* = 1 (the case here), if *n* differs, so will R<sup>2</sup>, and hence R<sup>2</sup><sub>adjusted</sub>. The value of the latter being close to 1 demonstrates that the data fit very well with the proposed equation, in this case, with the second-order kinetic law.

$$R^2_{adjusted} = 1 - \left(1 - R^2\right) \left[\frac{n - 1}{n - (m - 1)}\right] \tag{6}$$

The rate coefficient values in Table 2 have been used to calculate the overall activation energy *E<sub>a</sub>* and the pre-exponential factor *Z* by means of the linearized Arrhenius law. It fits fairly well (R<sup>2</sup><sub>adjusted</sub> = 0.7855) with the four experimental ln(*k*) vs. 1/*T* values. Hence, *E<sub>a</sub>* = 73.35 ± 21.26 KJ/mole and ln(*Z*) = 27.01 ± 8.43 were obtained, pointing to the chemisorption of BAC as the main adsorption mechanism. Previously, similar [31] and opposite (physical sorption) findings [35] have been previously reported, mainly depending on the nature of the adsorbent but also on the initial adsorbate/adsorbent mass ratio.

The experiments carried out at a constant 25 °C and variable initial BAC/paper mass ratio generated the rate coefficient values presented in Figure 5. It shows that the overall adsorption process is favored by both low and high ratios. At low ones, the adsorption might be favored by the large number of available empty sorption sites, thus occurring faster. On the other hand, at high mass ratios, the concentration gradient of BAC between the liquid bulk phase and the adsorbent’s surface increases, favoring diffusion, hence raising the overall rate constant.

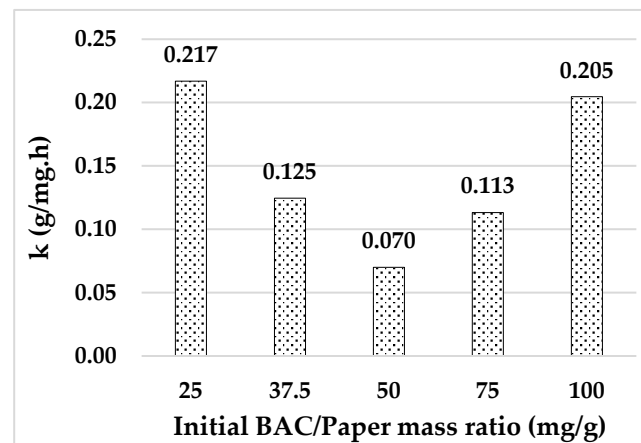


**Figure 5.** The dependence of overall pseudo-second-order rate coefficients  $k$  on the BAC/paper initial mass ratio, at  $25.0 \pm 0.1$  °C.

### 3.4. Adsorption Isotherms and Mechanism

The experiments carried out until equilibrium under the conditions described in Figure 5 led to the data presented in Table 3. It contains the equilibrium adsorption capacities  $q_{eq}$  (mg/g), which are quantitatively linked to the BAC retained on the adsorbent's surface as a function of their corresponding equilibrium remnant concentration in the liquid bulk phase,  $C_{eq}$  (mg/L). Both experimental and calculated  $q_{eq}$  values are provided. The latter are obtained from plots described through the use of Equation (5) and exemplified by Figure 3b. There is a very good match between the  $q_{eq}$  value pairs. Hence, (i) the suitability of the second-order kinetic model is reinforced since the slope of its linearized form (5) serves for the determination of  $q_{eq}$  calculated and (ii) the good quality of the experimental data is proven (see also the corresponding excellent  $R^2_{adjusted}$  values).

**Table 3.** Equilibrium data: BAC adsorption capacities  $q_{eq}$  (mg/g) vs. their corresponding equilibrium remnant concentration in the liquid bulk phase,  $C_{eq}$  (mg/L). Experimental and calculated data, at  $25 \pm 0.1$  °C.

$C_{eq}$ (mg/L)	$q_{eq}$ —Experimental (mg/g)	$q_{eq}$ —Calculated (mg/g)	$R^2_{adjusted}$
$63.63 \pm 4.03$	$18.64 \pm 0.02$	$18.69 \pm 0.04$	0.9980
$135.98 \pm 2.09$	$23.90 \pm 0.07$	$23.87 \pm 0.02$	0.9998
$264.36 \pm 2.11$	$23.56 \pm 1.04$	$23.53 \pm 1.01$	0.9997
$477.76 \pm 9.13$	$27.22 \pm 0.01$	$27.25 \pm 0.01$	0.9993
$672.30 \pm 11.17$	$32.77 \pm 1.05$	$33.33 \pm 0.07$	0.9980

Despite the fact that only the Langmuir [32,34,37] and Freundlich [30] isotherms are mentioned in the literature, the fitting quality of eight different adsorption isotherms [47–50] over these data was evaluated in order to decide upon one that might elucidate the process mechanism. Four models have two parameters (Langmuir, Freundlich, Dubinin-Radushkevich and Temkin), and four have three (Hill, Redlich–Peterson, Toth, and Radke–Prausnitz), respectively (see also Table 4).

**Table 4.** Equations, parameters and error function values for the tested adsorption isotherm models.

Model <sup>1,2</sup>	Equation	Parameters <sup>3</sup>	RMSD	HYBRID	R <sup>2</sup> <sub>adjusted</sub>
Langmuir <sup>1</sup>	$q = \frac{q_{max}K_L C_{eq}}{1+K_L C_{eq}}$	q <sub>max</sub> = 35.088 K <sub>L</sub> = 11.760	2.777	56.052	0.956
Freundlich <sup>1</sup>	$q = K_F C_{eq}^{\frac{1}{n}}$	K <sub>F</sub> = 7.900 n = 4.762	1.719	18.135	0.886
Dubinin–Radushkevich <sup>1</sup>	$q = q_s \exp(-k_{ad} \epsilon^2)$	q <sub>s</sub> = 3.10 <sup>-4</sup> k <sub>ad</sub> = 27.719	3.079	53.815	0.674
Temkin <sup>1</sup>	$q = \frac{RT}{b_T} \ln(A_T C_{eq})$	b <sub>T</sub> = 472.270 A <sub>T</sub> = 0.530	1.861	21.275	0.852
Hill <sup>2</sup>	$q = \frac{q_{sH} C_e^{n_H}}{k_D + C_e^{n_H}}$	q <sub>sH</sub> = 7191.3 k <sub>D</sub> = 744.214 n <sub>H</sub> = 0.168	2.268	41.914	0.865
Redlich–Peterson <sup>2</sup>	$q = \frac{K_R C_e}{1+a_R C_e^g}$	K <sub>R</sub> = 3673.7 a <sub>R</sub> = 464.983 g = 0.790	1.720	27.914	0.988
Toth <sup>2</sup>	$q = \frac{K_T C_{eq}}{(a_T + C_{eq})^t}$	K <sub>T</sub> = 7.492 a <sub>T</sub> = 0 t = 1.266	1.707	27.388	0.848
Radke–Prausnitz <sup>2</sup>	$q = \frac{a_{RP} K_{RP} C_{eq}^{\beta_R}}{a_{RP} + K_{RP} C_{eq}^{\beta_R - 1}}$	a <sub>RP</sub> = 3112.800 K <sub>RP</sub> = 7.493 β <sub>R</sub> = 0.220	1.708	27.504	0.857

<sup>1</sup> Two-parameter adsorption isotherm models. <sup>2</sup> Three-parameter adsorption isotherm models. <sup>3</sup> Units of parameters for the isotherms, whith the calculus performed with C<sub>eq</sub> values expressed in g/L: Langmuir—q<sub>max</sub> (mg/g) maximum monolayer coverage, K<sub>L</sub> (L/g) adsorption equilibrium constant; Freundlich—K<sub>F</sub> (mg/g) approximate indicator of adsorption capacity, n (dimensionless), with 1/n indicating adsorption strength, a model coefficient; Dubinin–Radushkevich—q<sub>s</sub> (mg/g) theoretical saturation capacity, k<sub>ad</sub> (mole<sup>2</sup>/KJ<sup>2</sup>) a measure of adsorption equilibrium constant, ε (dimensionless) Dubinin–Radushkevich isotherm constant, a model coefficient; Temkin—A<sub>T</sub> (mg/g) binding constant, b<sub>T</sub> (dimensionless) Temkin isotherm constant; Hill—q<sub>sH</sub> (mg/g) Hill saturation capacity, k<sub>D</sub> (L/g) Hill–Deboer isotherm constant, n<sub>H</sub> (dimensionless) model coefficient; Redlich–Peterson—K<sub>R</sub> (L/g) Redlich–Peterson isotherm constant, a<sub>R</sub> (g/mg) a measure of maximum adsorption capacity, g (dimensionless) model exponent with values between 0 and 1; Toth—K<sub>T</sub> (L/g) Toth isotherm constant, a<sub>T</sub> (mg/g) maximum adsorption capacity, t (dimensionless) heterogeneity factor; Radke–Prausnitz—a<sub>RP</sub> (mg/g) maximum adsorption capacity, K<sub>RP</sub> (L/g) Radke–Prausnitz isotherm constant, β<sub>R</sub> (dimensionless) model exponent.

The Langmuir model describes the ideal situation for which all adsorption sites are homogeneous in structure and, therefore, energetically equivalent. The adsorption is assumed to take place in a monolayer, one site at a time, only through chemisorption, without any consequences on the neighboring positions of an occupied site. Its equation is presented in Table 4. Its linearized form in Equation (7) permits the easy calculus of both the maximum adsorption capacity of a single layer at a given temperature, q<sub>max</sub> (mg/g), and the adsorption equilibrium constant at that temperature, K<sub>L</sub> (L/mg).

$$\frac{C_{eq}}{q_{eq}} = \frac{C_{eq}}{q_{max}} + \frac{1}{K_L q_{max}} \tag{7}$$

The data presented in Table 3 fitted well Equation (7), with R<sup>2</sup><sub>adjusted</sub> = 0.9562. Hence, at the standard temperature of 298 K, the following were obtained: q<sub>max</sub> = 35.09 mg/g and K<sub>L</sub> = 11.76 L/g, respectively.

However, despite being easy, the use of simple linear regressions to evaluate the fitting quality and to calculate the parameters of a model can generate significant errors. Moreover, it is limited to models that allow linearization. Therefore, the parameters of the eight isotherms were calculated by means of an optimization algorithm in MatLab Software. This works with the normalized mean square error (NMSE) as an objective function and strives to find its minimum. Its expression is provided in Equation (8). q<sub>exp(i)</sub> and q<sub>calc(i)</sub> stand for the i<sup>th</sup> experimental and calculated q values, respectively. The denominator

represents the average value of  $q_{exp}$ , and  $n$  is the number of experiments (here  $n = 5$ ). The decision variables of the objective function are the sought-after model parameters.

$$NMSE = \frac{\sqrt{\frac{\sum_{i=1}^n (q_{exp(i)} - q_{calc(i)})^2}{n}}}{\bar{q}_{exp}} \quad (8)$$

After finding the parameters of each adsorption isotherm, three more error functions were calculated as simultaneous tools to be used when deciding upon the best model: (1) RMSD function (root mean squared deviations), see Equation (9), (2) HYBRID function (hybrid fractional error deviation), see Equation (10) in which  $p$  is the number of parameters of the model [42,50], and (3)  $R^2_{adjusted}$ , see Equation (6).

$$RMSD = \sqrt{\frac{\sum_{i=1}^n (q_{exp(i)} - q_{calc(i)})^2}{n}} \quad (9)$$

$$HYBRID = \frac{100}{n-p} \sum_{i=1}^n \left( \frac{q_{exp(i)} - q_{calc(i)}}{q_{exp(i)}} \right)^2 \quad (10)$$

Table 4 lists the calculus results for the eight isotherms taken into consideration: the value of their parameters as well as of the three above-mentioned error functions. The footnotes indicate the units of the parameters for each isotherm [49,50]. A good quality fit simultaneously satisfies the following requests:  $R^2_{adjusted}$  as close to 1 as possible, whereas RMSD and HYBRID ought to be as close to zero as possible.

The analysis of the values in Table 4 suggests that the models fitting the best data in Table 3 are the Redlich–Peterson (RP) isotherm (lowest RMSD, relatively low HYBRID, very good  $R^2_{adjusted}$  of 0.988), seconded by the Langmuir (L) isotherm (best  $R^2_{adjusted}$ , yet weakest HYBRID), respectively. A comparison between the experimental values of  $q_{eq}$  and those calculated by these two models is presented in Figure 6. Both seem to do a good job (see also results of Table 4); however, the L-isotherm predicts values that are scattered among the experimental ones, whereas the RP-equation predicts lower  $q_{eq}$  values, regardless of the  $C_{eq}$  level. Hence, despite the better statistical error functions of the RP model, the Langmuir one still holds best. Similar conclusions have been previously reported [32,34,37].

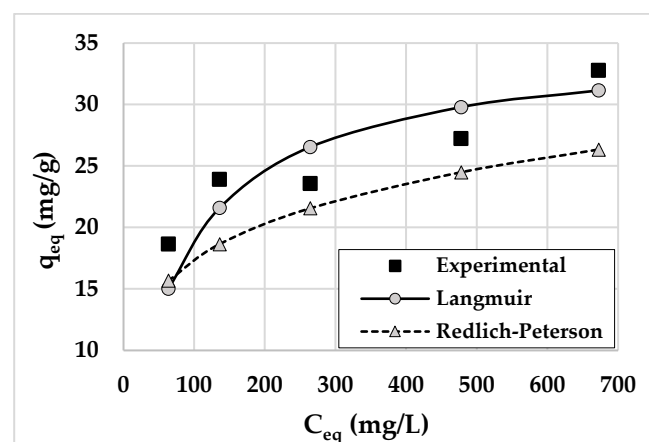


**Figure 6.** Experimental equilibrium isotherm data *vs.* calculated data for the Langmuir and Redlich–Peterson isotherms, respectively, at  $25.0 \pm 0.1$  °C.

The RP isotherm combines the characteristics of both the Langmuir and Freundlich (F) ones [48,49]. Unlike the L-model, it does not assume ideal monolayer adsorption. The equation in Table 4 shows that when the parameter  $g = 1$ , it will reduce to the Langmuir relationship. On the other hand, at high liquid-phase adsorbate concentrations or low  $g$  values, the model reduces to the F-isotherm. In this case, the value of  $g = 0.780$  shows a stronger similarity with the L-model. This fact also supports the conclusions reached in Figure 6.

Kim *et al.* [37] mention somewhat different sorption mechanisms for various BAC molecules: electrostatic interaction seems to be more significant in the case of BAC-12, whereas van der Waals bonding is more relevant for BAC molecules with longer alkyl chains. Since this study was carried out with a mixture of BAC-12 and BAC-14 in an unknown ratio, the equilibrium data describe a rather overall process, which seems to mainly follow chemisorption, with some physisorption (condensation) going on at high BAC concentrations: after completion of the monolayer, further BAC molecules can still attach themselves to the adsorbent's surface *via* Van der Waals bonding to the previous layers.

These conclusions are supported by the findings of Zanini *et al.* [31], who studied the synergistic effect of BAC-12 and BAC-14 when simultaneously adsorbed from mixtures. An isotherm with two well-differentiated steps was proposed, each corresponding to a different adsorption mechanism. These impregnate a letter S-shaped  $q_{eq}$  vs.  $C_{eq}$  plot, each plateau (leveling off) corresponding to a step: the first being explained by chemical and the second by physical processes. The experimental data in Figure 6 exhibit such a shape somewhat, with a leveling off in the 100–320 mg/L  $C_{eq}$  domain. However, there are too few points to correctly apply a double L-model (a sum of two terms, like the Langmuir equation presented in Table 4) [31], with four parameters to be determined from only five  $q_{eq}$ – $C_{eq}$  pairs.

It is possible to estimate the Gibbs free energy of adsorption  $\Delta G^0$  by using the Van't Hoff relationship (11) and the value of the equilibrium constant; however, the latter ought to be dimensionless [51].

$$\Delta G^0 = -RT \ln K_e^0 \quad (11)$$

Yet, the  $K_L = 11.76$  L/g provided by the Langmuir model is not dimensionless. Equation (12) [51] describes a way of computing the dimensionless equilibrium constant  $K_e^0$  in such cases:

$$K_e^0 = K_L \cdot \frac{[\text{adsorbate}]/[\text{adsorbate}]^0}{\gamma} \quad (12)$$

The  $[\text{adsorbate}]/[\text{adsorbate}]^0 = 353.5$  g/mole is the dimensionless standardized average molar mass of the employed BAC-12 and BAC-14 mixture (the ratio is unspecified by the provider; however, for the sake of this calculus, a 1:1 value was considered);  $\gamma$  is the activity coefficient, which was here considered to be equal to 1. The obtained  $K_e^0$  value enabled the calculus of  $\Delta G^0$  with the help of (11) ( $R = 8.314$  J/mole·K,  $T = 298$  K).

The resulting value of the  $\Delta G^0 = -20.64$  KJ/mole indicates a spontaneous process at 298 K. The magnitude of this adsorption free energy is comparable to those reported for other cationic adsorbates [52], yet it is approximately five-fold higher than values reported for BAC physisorption on powdered activated carbon [37]. Hence, again, a somewhat hybrid chemi- and physisorption mechanism may be assumed for the adsorption of BAC on the studied household paper.

This study proposes a low-cost, unmodified adsorbent for benzalkonium chloride from its aqueous solutions prepared by using a commercial mixture of BAC-12 and BAC-14. Both are readily accessible to the general public, both in terms of availability as well as price. Even so, the achieved adsorption capacities at 25 °C are comparable to the ones mentioned previously for another low-cost adsorbent: 11 ÷ 22 mg/g on polyethylene microplastics [40]. On the other hand, up to one order of magnitude higher values of (100 to 500 mg/g) may be targeted when using activated carbon [30,37] or montmorillonite [31,33,36,38].

However, these require complex and pricey physical and chemical treatment prior to their employment as adsorbents.

#### 4. Conclusions

This study had the following aims: (1) to elucidate whether various low-cost household materials are suitable, in their unmodified and untreated form, to effectively adsorb benzalkonium chloride from its aqueous solutions and (2) to elucidate the process kinetics and thermodynamics of BAC adsorption on the proper adsorbent.

Among the five investigated adsorbents, household paper was chosen to be the most suitable for further testing in standardized batch experiments. Variation of both temperature and initial adsorbate/adsorbent mass ratio affected the adsorption capacity *vs.* the S-L contact time profile, with the latter being the stronger factor.

Four different kinetic models were tested, yet only the pseudo-second-order law fitted the data. Calculated rate coefficients lead to an apparent activation energy, which suggests that the removal of BAC occurs by means of chemisorption. Low and high initial BAC amounts in the sample speed up the process, which is either due to available adsorbent empty sites or the higher concentration gradient between the solid and liquid phases, respectively.

Equilibrium data at 25 °C were tested against eight isotherms. Their parameters were determined by minimizing the normalized mean square error. The data fitting quality was assessed through the use of three simultaneously employed statistical error functions. Both the Langmuir and the Redlich–Peterson isotherm were good fits, with the former being somewhat better scattered among the experimental values. The negative and medium-sized value of the Gibbs free energy suggested hybrid chemical and physical adsorption.

The study proved that even readily available, unmodified, and untreated household materials can be used as efficient adsorbents for the rapid removal of benzalkonium chloride, a biocide with many use yet which poses increasing ecological concerns.

**Author Contributions:** Conceptualization, E.B. and A.C.; methodology, A.C.; software, A.C.; validation, A.C.; formal analysis, E.B.; investigation, A.C.; resources, E.B. and A.C.; data curation, A.C.; writing, original draft preparation, A.C.; writing, review and editing, A.C.; visualization, E.B. and A.C.; supervision, E.B.; project administration, E.B. All authors have read and agreed to the published version of the manuscript.

**Funding:** This research was funded by the Transylvanian Museum Society, Cluj-Napoca, Romania, Grant-number 220.11.1/2020. The APC was funded by the Transylvanian Museum Society, Cluj-Napoca, Romania, and the Babeş-Bolyai University of Cluj-Napoca, Romania.

**Institutional Review Board Statement:** Not applicable.

**Informed Consent Statement:** Not applicable.

**Data Availability Statement:** The data presented in this study are available upon request from the corresponding author.

**Acknowledgments:** The authors thank the Research Institute of the Transylvanian Museum Society, Cluj-Napoca, Romania, for its kind logistical support, as well as chemical engineer Lascu Ana-Maria (born Danciu) for her kind help during the experimental work.

**Conflicts of Interest:** The authors declare no conflict of interest.

#### References

1. Ahuja, K.; Bayas, S. Benzalkonium Chloride Market Size by Type (Benzalkonium Chloride 80%, Benzalkonium Chloride 50%), by Application (Biocide [Water Treatment Chemical, Disinfectant, Preservative], Phase Transfer Catalyst), by End-Use (Food & Beverage, Cosmetics, Polymers & Coatings, Pharmaceuticals, Chemical Industry, Pulp and Paper, Leather & Textile, Oil & Gas), Industry Analysis Report, Regional Outlook, Growth Potential, Price Trend, Competitive Market Share & Forecast, 2021–2027. Global Market Insights; Report ID: GMI3233. 2021. Available online: <https://www.gminsights.com/industry-analysis/benzalkonium-chloride-market> (accessed on 30 October 2023).

2. Zhang, C.; Tezel, U.; Li, K.; Liu, D.; Ren, R.; Du, J.; Pavlostathis, S.G. Evaluation and Modeling of Benzalkonium Chloride Inhibition and Biodegradation in Activated Sludge. *Water Res.* **2011**, *45*, 1238–1246. [[CrossRef](#)] [[PubMed](#)]
3. Nan, H.; Wang, T.; Wang, W.L.; Wu, Q.Y.; Li, A.; Hu, H.Y. UV/Chlorine as an Advanced Oxidation Process for the Degradation of Benzalkonium Chloride: Synergistic Effect, Transformation Products and Toxicity Evaluation. *Water Res.* **2017**, *114*, 246–253.
4. Abott, T.; Kor-Bicakci, G.; Islam, M.S.; Eskicioglu, C. A Review on the Fate of Legacy and Alternative Antimicrobials and Their Metabolites during Wastewater and Sludge Treatment. *Int. J. Mol. Sci.* **2020**, *21*, 9241. [[CrossRef](#)]
5. Kim, S.; Ji, K.; Shin, H.; Park, S.; Kho, Y.; Park, K.; Kim, K.; Choi, K. Occurrences of Benzalkonium Chloride in Streams Near a Pharmaceutical Manufacturing Complex in Korea and Associated Ecological Risk. *Chemosphere* **2020**, *256*, 127084. [[CrossRef](#)]
6. Barber, O.W.; Hartmann, E.M. Benzalkonium chloride: A Systematic Review of Its Environmental Entry through Wastewater Treatment, Potential Impact, and Mitigation Strategies. *Crit. Rev. Environ. Sci. Technol.* **2022**, *52*, 2691–2719. [[CrossRef](#)]
7. Fuchsman, P.; Fetters, K.; O'Connor, M.; Henning, M.; Brown, L.; Mrdjen, I.; Stanton, K. Ecological Risk Analysis for Benzalkonium Chloride, Benzethonium Chloride, and Chloroxylenol in US Disinfecting and Sanitizing Products. *Environ. Toxicol. Chem.* **2022**, *41*, 3095–3115. [[CrossRef](#)]
8. Sreevidya, V.S.; Lenz, K.A.; Svoboda, K.R.; Ma, H. Benzalkonium Chloride, Benzethonium Chloride, and Chloroxylenol—Three Replacement Antimicrobials are More Toxic than Triclosan and Triclocarban in Two Model Organisms. *Environ. Pollut.* **2018**, *235*, 814–824. [[CrossRef](#)] [[PubMed](#)]
9. Ikisa, K.G.; Banatunde, B.B.; Hart, A.I. Acute Toxicity of Benzalkonium Chloride Mixture with Treated Produced Water to Juveniles of Freshwater Tilapia- *Oreochromis niloticus*. *J. Appl. Sci. Environ. Manag.* **2019**, *23*, 1169–1174. [[CrossRef](#)]
10. Lavorgna, M.; Russo, C.; D'Abrosca, B.; Parrella, A.; Isidori, M. Toxicity and Genotoxicity of the Quaternary Ammonium Compound Benzalkonium Chloride (BAC) Using *Daphnia magna* and *Ceriodaphnia dubia* as Model Systems. *Environ. Pollut.* **2016**, *210*, 34–39. [[CrossRef](#)]
11. Perez, P.; Fernandez, E.; Beiras, R. Toxicity of Benzalkonium Chloride on Monoalgal Cultures and Natural Assemblages of Marine Phytoplankton. *Water Air Soil. Pollut.* **2009**, *201*, 319–330. [[CrossRef](#)]
12. Sousa, B.; Domingues, I.; Nunes, B. A Fish Perspective on SARS-CoV-2: Toxicity of Benzalkonium Chloride on *Danio rerio*. *Environ. Toxicol. Pharmacol.* **2023**, *102*, 104200. [[CrossRef](#)]
13. *Benzalkonium Chloride, Safety Data Sheet*; Spectrum Chemical Mfg. Corp.: Gardena, CA, USA, 2022; p. 7.
14. *Benzalkonium Chloride 50%, Safety Data Sheet*; Fisher Scientific Company: Fair Lawn, NJ, USA, 2021; pp. 2, 5–6.
15. *Benzalkonium Chloride 80%, Safety Data Sheet*; Laboratoriumdiscounter: Ijmuiden, The Netherlands, 2023; pp. 2, 4–5.
16. Tezel, U.; Giles, H.; deRussy, A.; Pavlostathis, S.G. Effect of Counter Ions and Natural Organic Matter on the Toxicity of Benzalkonium Chloride. *Proc. Water Environ. Fed.* **2009**, *17*, 621–631. [[CrossRef](#)]
17. Sahoo, T.R.; Prelot, B. Adsorption Processes for the Removal of Contaminants from Wastewater: The Perspective Role of Nanomaterials and Nanotechnology. In *Nanomaterials for the Detection and Removal of Wastewater Pollutants*; Bonelli, B., Freyria, F.S., Rossetti, I., Sethi, R., Eds.; Elsevier: Amsterdam, The Netherlands, 2021; Chapter 7; pp. 161–222.
18. Krstić, V. Role of Zeolite Adsorbent in Water Treatment. In *Handbook of Nanomaterials for Wastewater Treatment: Fundamentals and Scale Up Issues*; Bhanvase, B., Sonawane, S., Pawade, V., Pandi, A., Eds.; Elsevier: Amsterdam, The Netherlands, 2021; Chapter 14; pp. 417–481.
19. Meez, E.; Rahdar, A.; Kyaz, G.Z. Sawdust for the Removal of Heavy Metals from Water: A Review. *Molecules* **2021**, *26*, 4318. [[CrossRef](#)] [[PubMed](#)]
20. Hassan, M.M.; Carr, C.M. Biomass-derived Porous Carbonaceous Materials and Their Composites as Adsorbents for Cationic and Anionic Dyes: A Review. *Chemosphere* **2021**, *265*, 129087. [[CrossRef](#)] [[PubMed](#)]
21. Yagub, M.T.; Sen, T.K.; Afroze, S.; Ang, H.M. Dye and Its Removal from Aqueous Solution by Adsorption: A Review. *Adv. Colloid. Interface Sci.* **2014**, *209*, 172–174. [[CrossRef](#)] [[PubMed](#)]
22. Sahmoune, M.N.; Yeddou, A.R. Potential of Sawdust Materials for the Removal of Dyes and Heavy Metals: Examination of Isotherms and Kinetics. *Desalin. Water Treat.* **2016**, *57*, 24019–24034. [[CrossRef](#)]
23. Chikri, R.; Elhadiri, N.; Bechanaa, M.; El Maguana, Y. Efficiency of Sawdust as Low-Cost Adsorbent for Dyes Removal. *J. Chem.* **2020**, *2020*, 8813420. [[CrossRef](#)]
24. Markovic, R.; Stevanovic, J.; Stevanovic, Z.; Bugarin, M.; Nedeljkovic, D.; Grujic, A.; Stajic-Trosic, J. Using the Low-Cost Waste Materials for Heavy Metals Removal from the Mine Wastewater. *Mater. Trans.* **2011**, *52*, 1849–1852. [[CrossRef](#)]
25. Dorri, Y.; Kurien, B.T. Paper Adsorbents Remove Coomassie Blue from Gel Destain and Used Gel Stain in an Environment-Friendly Manner. *Methods Mol. Biol.* **2018**, *1853*, 259–268.
26. Diaz-Linan, M.C.; Lucena, R.; Cardenas, S.; Lopez-Lorente, A.I. Unmodified Cellulose Filter Paper, a Sustainable and Affordable Sorbent for the Isolation of Biogenic Amines from Beer Samples. *J. Chromatogr. A* **2021**, *1651*, 462297. [[CrossRef](#)]
27. Nabais, J.M.V.; Laguinhas, C.E.; Román, S. Biomass Novel Adsorbents for Phenol and Mercury Removal. *Molecules* **2022**, *27*, 7345. [[CrossRef](#)] [[PubMed](#)]
28. Vancea, C.; Mladin, G.; Ciopec, M.; Negrea, A.; Duteanu, N.; Negrea, P.; Mosoarca, G.; Ianasi, C. Arsenic Removal Using Unconventional Material with Iron Content: Batch Adsorption and Column Study. *Toxics* **2023**, *11*, 849. [[CrossRef](#)] [[PubMed](#)]
29. Wu, Y.; Sang, H.; Zheng, J.; Yang, S.; Gu, Z.; Wu, H.; Wei, Y. Preparation and Density Functional Theory Studies of Aluminosilicate-Based Ceramic Solidified Products for Sr Immobilization. *Toxics* **2023**, *11*, 850. [[CrossRef](#)] [[PubMed](#)]

30. Tanada, M.; Miyoshi, T.; Nakamura, T.; Tanada, S. Adsorption Removal of Benzalkonium Chloride by Granular Activated Carbon for Medical Waste Water Treatment. *Asia Pac. J. Public Health* **1991**, *5*, 27–31. [[CrossRef](#)]
31. Zanini, G.P.; Ovesen, R.G.; Hansen, H.C.B.; Strobel, B.W. Adsorption of the Disinfectant Benzalkonium Chloride on Montmorillonite. Synergistic Effect in Mixture of Molecules with Different Chain Lengths. *J. Environ. Manag.* **2013**, *128*, 100–105. [[CrossRef](#)]
32. Ong, L.K.; Soetaredjo, F.E.; Kurniawan, A.; Ayucitra, A.; Liu, J.-C.; Ismadji, S. Investigation on the Montmorillonite Adsorption of Biocidal Compounds Incorporating Thermodynamical-Based Multicomponent Adsorption Isotherm. *J. Chem. Eng.* **2014**, *241*, 9–18. [[CrossRef](#)]
33. Ilari, R.; Etcheverry, M.; Waiman, C.V.; Zanini, G.P. A Simple Cation Exchange Model to Assess the Competitive Adsorption between the Herbicide Paraquat and the Biocide Benzalkonium Chloride on Montmorillonite. *Colloids Surf. A Physicochem. Eng. Asp.* **2021**, *611*, 125797. [[CrossRef](#)]
34. Paun, I.; Covaliu, C.I.; Pirvu, F.; Paraschiv, G.; Nita-Lazar, M. Benzalkonium Bromide Cationic Surfactant Removal from Wastewater Using Magnetite Nanomaterial. *Rev. Chim.* **2020**, *71*, 289–296. [[CrossRef](#)]
35. Turku, I.; Sainio, T.; Paatero, E. Removal of Benzalkonium Chloride by Polymeric Adsorbents. In Proceedings of the Book of Abstracts European Congress of Chemical Engineering (ECCE-6), Copenhagen, Denmark, 16–20 September 2007.
36. Kim, T.-K.; Jang, M.; Hwang, Y.S. Adsorption of Benzalkonium Chlorides onto Polyethylene Microplastics: Mechanism and Toxicity Evaluation. *J. Hazard. Mater.* **2022**, *426*, 128076. [[CrossRef](#)]
37. Kim, T.-K.; Choe, W.-S.; Kim, T.; Chae, S.-H.; Hwang, J.S.; Zoh, K.-D. Adsorption of benzalkonium chlorides onto powdered activated carbon: Mechanisms and detoxification. *Environ. Eng. Res.* **2022**, *27*, 210496. [[CrossRef](#)]
38. do Nascimento, D.S.; Etcheverry, M.; Orduz, E.A.; Waiman, C.V.; Zanini, G.P. Adsorption of cationic surfactant as a probe of the montmorillonite surface reactivity in the alginate hydrogel composites. *RSC Adv.* **2022**, *12*, 35469–35476. [[CrossRef](#)] [[PubMed](#)]
39. Farias, T.; de Mênorval, L.C.; Zajac, J.; Rivera, A. Benzalkonium Chloride and Sulfamethoxazole Adsorption onto Natural Clinoptilolite: Effect of Time, Ionic Strength, pH and Temperature. *J. Colloid. Interface Sci.* **2011**, *363*, 465–475. [[CrossRef](#)] [[PubMed](#)]
40. Bin, T.; Kulshreshtha, A.K.; Al-Shakhshir, R.; Hem, S.L. Adsorption of Benzalkonium Chloride by Filter Membranes: Mechanisms and Effect of Formulation and Processing Parameters. *Pharm. Dev. Technol.* **1999**, *4*, 151–165. [[CrossRef](#)] [[PubMed](#)]
41. Peshovska, V.; Atanaskova, E.; Cholakova, I.; Stojanovska, N.A.; Angelovska, V.; Mojsovska, M. Selectopn of Filter for Sterilization Using Process of Membrane Filtration Based on Potential Adsorption of Benzalkonium Chloride on Filter Membranes. In Proceedings of the 7th Conference on Pharmacy (Modern Trends in Pharmacy, Opportunities and Challenges), Ohrid, Macedonia, 5–9 October 2022.
42. Šćiban, M.; Klačnja, M.; Škrbić, B. Modified Softwood Sawdust as Adsorbent of Heavy Metal Ions from Water. *J. Hazard. Mater.* **2006**, *136*, 266–271. [[CrossRef](#)]
43. Argun, M.E.; Dursun, S.; Ozdemir, C.; Karatas, M. Heavy Metal Adsorption by Modified Oak Sawdust: Thermodynamics and Kinetics. *J. Hazard. Mater.* **2007**, *141*, 77–85. [[CrossRef](#)]
44. Ellison, S.L.R.; Barwick, V.J.; Farrant, T.J.D. *Practical Statistics for the Analytical Scientist*, 2nd ed.; RSC Publishing: Cambridge, UK, 2009; pp. 59–65, 92–108.
45. Csavdari, A.A. Detailed Kinetics of a Diffusion Driven Adsorption Process. *Stud. Univ. Babeş-Bolyai Chem.* **2023**, *68*, 179–189.
46. Joglekar, A.M.; May, A.T. Product Excellence through Design of Experiments. *CFW* **1987**, *32*, 857–868.
47. Rahman, M.M.; Muttakin, M.; Pal, A.; Shafiullah, A.Z.; Saha, B.B. A Statistical Approach to Determine Optimal Models for IUPAC-Classified Adsorption Isotherms. *Energies* **2019**, *12*, 4565. [[CrossRef](#)]
48. Al-Ghouti, M.A.; Da’ana, D.A. Guidelines for the Use and Interpretation of Adsorption Isotherm Models: A Review. *J. Hazard. Mater.* **2020**, *393*, 122383. [[CrossRef](#)]
49. Dada, A.O.; Olalekan, A.P.; Olatunya, A.M.; Dada, O. Langmuir, Freundlich, Temkin and Dubinin–Radushkevich Isotherms Studies of Equilibrium Sorption of Zn<sup>2+</sup> Unto Phosphoric Acid Modified Rice Husk. *IOSR-JAC* **2012**, *3*, 38–45.
50. Serafin, J.; Dziejarski, B. Application of Isotherm Models and Error Functions in Activated Carbon CO<sub>2</sub> sorption processes. *Microporous Mesoporous Mater.* **2023**, *354*, 112513. [[CrossRef](#)]
51. Lima, E.C.; Hosseini-Bandegharai, A.; Moreno-Pirajan, J.C.; Anastopoulos, I. A Critical Review of the Estimation of the Thermodynamic Parameters on Adsorption Equilibria. Wrong Use of Equilibrium Constant in the Van’t Hoff Equation for Calculation of Thermodynamic Parameters of Adsorption. *J. Mol. Liq.* **2019**, *273*, 425–434. [[CrossRef](#)]
52. Saha, P.; Chowdhury, S. Insight into Adsorption Thermodynamics. In *Thermodynamics*; Tadashi, M., Ed.; INTECH: Rijeka, Croatia, 2011; Chapter 16; pp. 349–364.

**Disclaimer/Publisher’s Note:** The statements, opinions and data contained in all publications are solely those of the individual author(s) and contributor(s) and not of MDPI and/or the editor(s). MDPI and/or the editor(s) disclaim responsibility for any injury to people or property resulting from any ideas, methods, instructions or products referred to in the content.